PCCP

Accepted Manuscript

ROYAL SOCIETY OF CHEMISTRY

www.rsc.org/pccp

Cite this: DOI: 10.1039/c0xx00000x

www.rsc.org/xxxxxx

ARTICLE TYPE

Protonation induced shifting of electron-accepting center in intramolecular charge transfer chromophores and theoretical study†

Tao Tang,[a] Hong Chi,[c] Tingting Lin,[b] FuKe Wang,*[b,c] and Chaobin He,*[a,b]

Received (in XXX, XXX) Xth XXXXXXXXX 20XX, Accepted Xth XXXXXXXXX 20XX

DOI: 10.1039/b000000x

A new series of chameleonic molecules containing azulene and benzothiadiazole (**BT**) were designed and synthesized. In the neutral state, **BT** functions as electron accepting center, while under protonation, the electron accepting center shifts to azulene moieties, leading to a remarkable extension of absorption to NIR region, i.e. up to 2.5 um. The interchange between donor and acceptor characters upon protonation was confirmed by UV-vis-NIR spectra studies and supported by DFT calculation. Furthermore, HOMO-LUMO level of ICT chromophores could be finely tailored by different arrangement of azulenes and **BT**s in the molecules. The interchange between donor and acceptor characters upon protonation provides an alternative and yet effective approach to tune optical and electronic properties of NIR chromophores.

Introduction

Organic chromophores with narrow band gap have found many applications in near infrared (NIR) fluorophores,[1-3] photovoltaics,[4-6] NIR photo-detectors/optoelectronics,[7,8] and space telecommunications.[9,10] Several approaches have been devised to narrow the band gap of chromophores, such as increasing the conjugation length, using electron donors (D) and acceptors (A), and reducing the bond-length alternation of the conjugated backbones.[11,12] Among these strategies, the incorporation of D/A moieties to conjugated system is by far the most effective to tailor the optoelectronic properties of organic chromophores, since the combination of an electron-rich donor and an electron-deficient acceptor results in a comparable degrees of charge separation in the electronic ground state, and the intramolecular charge transfer (ICT) excited state reduce the excitation energy.[13-16] In this way, the optical and electric properties can be tailored by judicially design of the donor and acceptor structures.[17-19] For instance, molecules with triarylamines are most often used as electron donors.[20] Electron withdrawing groups/units such as cyanoacrylic acid and rhodanine-3-acetic acid,[21-23] tetracyanoethene (TCNE) and 7,7,8,8-tetracyanoquinodimethane (TCNQ) with several cyano groups are widely used as electron acceptors.[24,25] However, most of the electron acceptors in the reported ICT system are weak or moderate electron withdrawing groups/units, which limit their abilities to extend absorption spectra to above 1 μm.[26,27] Recently, we showed that azulene was a powerful electron-acceptor upon protonation, and a series of azulene containing polymers with tunable NIR absorption up to 2.5 um upon protonation have been reported.[28] In our previous work, we surprisingly found that the coupling of either electron donating moieties such as benzo-dithiophene or electron accepting moieties such as benzothiadiazole (**BT**) with azulene lead to similar ICT effect. The expected hypsochromic effect induced by the strong electron-accepting **BT** was not observed.

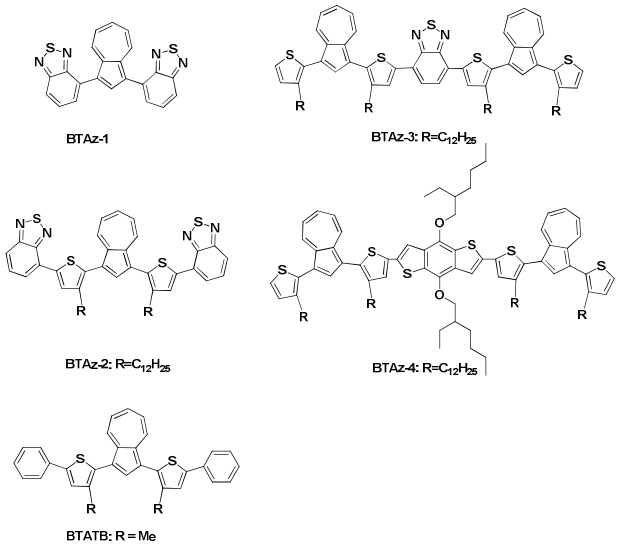

Scheme 1 Chemical structures of the azulene-containing conjugated compounds.

To gain insight into the ICT effect in **BT**-azulene system, and to find a new way to fine tuning the HOMO-LUMO band gap of the ICT chromophores, we herein report the design and synthesis of a new series of ICT systems which contain both azulene and **BT** as shown in Scheme 1. In neutral state of azulene and **BT** based systems, **BT** functions as electron-acceptor due to the existence of heteroatom interaction and azulene acts as electron-donor. Therefore, electron drift occurs from azulenes to **BT**s in the azulene-**BT**s conjugated molecules. However, when azulene was protonated and became azulenylium ion, the electron-accepting center moves to the protonated azulene, leading a new

ICT system. The shifting of electron accepting center induced by protonation explains the hypsochromic shift for **BT**-azulene containing polymer. Due to the extreme strong electron accepting characteristic of azulenylium ion, the main absorption could be extended to the telecommunications region, i.e. between 1300 nm to 2000 nm, which allows the chromophores to be used in NIR switching and space communications. Furthermore, it provides an alternative and effective approach to tune optical and electronic properties of chromophores. Generally, the functions of donor and acceptor for most reported NIR organic chromophores are fixed and not interchangeable. In our approach, we showed a simple way to build organic chromophore with chameleonic properties. That is, its optical properties can change with the environment characteristics. The protonation can shift its electron accepting center and thus lead to a remarkable optical properties change. Therefore, the systematic experimental and theoretical study of the optical properties of **BT**-azulene systems open a new way to build chameleonic molecules, as well as a better understanding of the ICT effect.

Experimental

Materials

Azulene (99%), 3-bromothiophene (97%), tri(o-tolyl)phosphine and magnesium turnings were purchased from Alfa Aesar. $Pd(dppf)Cl_2$, N-Bromosuccinimide(97%), 1-bromododecane (97%), 2,1,3-Benzothiadiazole (98%), bis(pinacolato)diboron (99%) and potassium acetate (99%) were purchased form Aldrich. $Ni(dppp)Cl_2$ and n-BuLi were purchased from Acros Organics. Compounds such as 3-alkyl-thiophene, 3-alkyl-2-bromothiophene, 1,3-Bis[2-(3-n-dodecylthienyl)]azulene, 1,3-Dibromo-[2-(3-dodecylthienyl)]azulene and 4-(4,4,5,5-tetramethyl-1,3,2-dioxaboralan-2-yl)-2,1,3-benzothiadiazole were prepared as depicted in the literatures with minor modifications.[29-31] Tetrahydrofuran (THF) was distilled from sodium benzophenone ketyl solution. Other commercially available solvents and reagents were used as received.

Computer Simulations

All calculations were performed with the Gaussian 09 program employing the Becke Three Parameter Hybrid Functionals Lee−Yang−Parr (B3LYP) in conjunction with the 6-31G(d) basis set.[32] Full geometry optimizations without symmetry constraints were carried out in the gas phase for the singlet ground states (S_0). The energies of highest occupied molecular orbital (HOMO), lowest unoccupied molecular orbital (LUMO) and other frontier orbitals were calculated at the optimized structure. The first fifty singlet–singlet transition energies and oscillation strengths for **BTAz**s were computed at the optimized S_0 geometries by using the time-dependent DFT (TD-DFT) methodology.[33] The excited states were calculated at the optimized ground state geometry using TD-DFT and at the same level of theory as ground state geometry optimization.

Synthesis of compounds

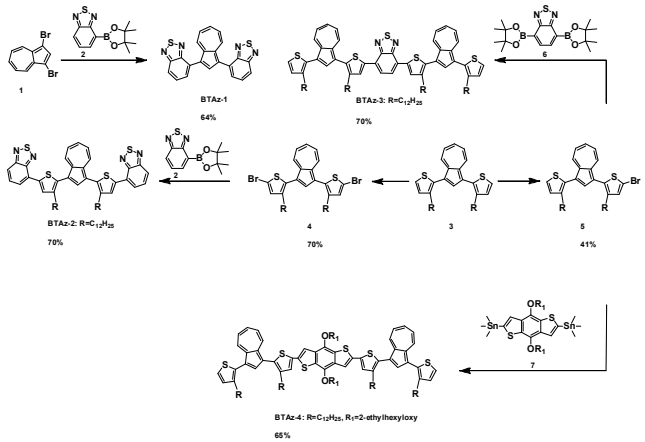

Scheme 2. The synthesis of the conjugated compounds.

1,3-bis(benzo[c][1,2,5]thiadiazol-4-yl)azulene (**BTAz-1**). To a two necked 50 ml RBF was added 1,3-dibomoazulene (**1**, 0.172 g, 0.6 mmol) and 4-(4,4,5,5-tetramethyl-1,3,2-dioxaboralan-2-yl)-2,1,3-benzothiadiazole (**2**, 0.33 g, 1.26 mmol), 8 ml of toluene, 4 ml of Na_2CO_3 solution (2 M), and 1 drop of Aliquat 336 under argon protection. The mixture was then vacuum degassed through several freeze-pump-thaw cycles for half hour. Catalytic amount of $Pd(PPh_3)_4$ (3.6 mg, 0.00312 mmol) was added and one more freeze-pump-thaw degas cycle was applied. The mixture was then transferred to an oil bath and stirred and refluxed at 100 °C for 24 hours. After cooling, the reaction mixture was extracted with toluene and the organic layers were collected, washed with water (three times) and dried over magnesium sulfate. After filtration, the volatile toluene was removed through rotary evaporator. The crude product was chromatographed on silica gel using hexane/DCM (4/1, v/v) as eluent followed by recrystallization from DCM to afford the title compound (64%) as brown powers. ^{1}H-NMR (δ, $CDCl_3$): 8.89 (s, 1 H), 8.63 (d, 2 H), 8.04 (d, 2 H), 7.85 (d, 2 H), 7.79 (t, 2 H), 7.73 (t, 1 H), 7.30 (t, 2 H). ^{13}C NMR: δ 156.1, 155.2, 141.3, 139.8, 138.9, 136.8, 130.7, 130.1, 129.8, 126.2, 125.3, 120.1. HRMS(APCI): calcd for $C_{22}H_{12}N_4S_4$, m/z 397.0537; found, m/z 397.0576.

1,3-bis(5-(benzo[c][1,2,5]thiadiazol-4-yl)-3-dodecylthiophen-2-yl)azulene (**BTAz-2**). To a two necked 50 ml RBF was added 1,3-Dibromo-[2-(3-dodecylthienyl)]azulene (**4**, 0.6 g, 0.76 mmol) and 4-(4,4,5,5-tetramethyl-1,3,2-dioxaboralan-2-yl)-2,1,3-benzothiadiazole (**2**, 0.42 g, 1. 6 mmol), 8 ml of toluene, 4 ml of Na_2CO_3 solution (2 M), and 1 drop of Aliquat 336 under argon protection. The mixture was then vacuum degassed through several freeze-pump-thaw cycles for half hour. Catalytic amount of $Pd(PPh_3)_4$ (4.5 mg, 0.0039 mmol) was added and one more freeze-pump-thaw degas cycle was applied. The mixture was then transferred to an oil bath and stirred and refluxed at 100 °C for 24 hours. After cooling, the reaction mixture was extracted with ethyl ether and the organic layers were collected, washed with water (three times) and dried over magnesium sulfate. After filtration, the volatile toluene and ethyl ether was removed through rotary evaporator. The crude product was chromatographed on silica gel using hexane/DCM (8/1, v/v) as eluent followed by recrystallization from hexane to afford the title compound (76%) as dark red color. ^{1}H-NMR (δ, $CDCl_3$):

8.54 (d, 2 H), 8.19 (s, 2 H), 8.07 (s, 1 H), 7.93 (m, 4 H), 7.66 (m, 3 H), 7.25 (t, 2 H), 2.70 (t, 4 H), 1.68 (t, 4 H), 1.24 (m, 36 H), 0.86 (t, 6 H). ^{13}C NMR: δ 156.1, 152.6, 142.2, 140.4, 139.7, 139.2, 138.4, 137.2, 134.3, 130.7, 130.1, 128.2, 125.3, 124.6, 122.2, 120.1, 32.3, 31.3, 30.1, 29.8, 23.1, 14.5. HRMS (APCI): calcd for $C_{54}H_{64}N_4S_4$, m/z 897.4047; found, m/z 897.4087.

5-bromo-3-dodecyl-2-(3-(3-dodecylthiophen-2-yl)azulen-1-yl)thiophene (**5**). NBS (0.346g, 1.94mmol) was added in portions to a solution of compound 1,3-Bis[2-(3-n-dodecylthienyl)]azulene (**3**, 1.22 g, 1.94 mmol) in $CHCl_3$/HOAC (10 ml/10 ml) at 0 °C over 45 minutes. The reaction was stirred for 1 hour at 0 °C and then at room temperature overnight. Stopped the reaction by addition of water and extracted with $CHCl_3$ (25 ml x 3). The organic layers were combined and washed with Na_2CO_3 solution; 50 ml water (three times) and dried over magnesium sulfate. After filtration, the volatile $CHCl_3$ was removed through rotary evaporator. The crude product was chromatographed on silica gel using hexane as eluent. This was obtained as blue oil (40%). ^{1}H-NMR (δ, $CDCl_3$): 8.39 (t, 2 H), 7.87 (s, 1 H), 7.66 (t, 1 H), 7.36 (d, 1 H), 7.22 (t, 2 H), 7.10 (d, 1 H), 7.04 (s, 1 H), 2.56 (m, 4 H), 1.17 (m, 36 H), 0.89 (m, 10 H). ^{13}C NMR: δ 141.7, 141.0, 140.5, 139.5, 139.1, 137.1, 136.7, 134.1, 132.1, 129.4, 124.9, 124.4, 122.5, 121.0, 111.0, 32.3, 31.3, 31.1, 30.0, 29.8, 29.6, 29.4, 23.1, 14.5. HRMS(APCI): calcd for $C_{42}H_{59}BrS_2$, m/z 708.3221; found, m/z 707.3314.

4,7-bis(4-dodecyl-5-(3-(3-dodecylthiophen-2-yl)azulen-1-yl)thiophen-2-yl)benzo[c][1,2,5]thiadiazole (**BTAz-3**). To a two necked 50 ml RBF was added 2,1,3-Benzothiadiazole-4,7-bis(boronic acid pinacol ester) (0.082 g, 0.21 mmol) and 5-bromo-3-dodecyl-2-(3-(3-dodecylthiophen-2-yl)azulen-1-yl)thiophene (**5**, 0.33g, 0.467 mmol), 4 ml of toluene, 2 ml of Na_2CO_3 solution (2 M), and 1 drop of Aliquat 336 under argon protection. The mixture was then vacuum degassed through several freeze-pump-thaw cycles for half hour. Catalytic amount of $Pd(PPh_3)_4$ (1.2 mg, 0.001 mmol) was added and one more freeze-pump-thaw degas cycle was applied. The mixture was then transferred to an oil bath and stirred and refluxed at 100 °C for 24 hours. After cooling, the reaction mixture was extracted with ethyl ether and the organic layers were collected, washed with water (three times) and dried over magnesium sulfate. After filtration, the volatile toluene and ethyl ether was removed through rotary evaporator. The crude product was chromatographed on silica gel using hexane/DCM (20/3) as eluent. This was obtained as red oil (70%). ^{1}H-NMR (δ, $CDCl_3$): 8.56 (d, 2 H), 8.42 (d, 2 H), 8.20 (s, 2 H), 8.01 (s, 2 H), 7.91 (s, 2 H), 7.65 (t, 2 H), 7.37 (d, 2 H), 7.22 (m, 4 H), 7.12 (d, 2 H), 2.67 (m, 8 H), 1.20 (m, 80 H), 0.88 (m, 12 H). ^{13}C NMR: δ 153.2, 142.2, 141.1, 140.6, 139.5, 139.3, 138.9, 138.5, 137.1, 134.4, 132.2, 130.3, 129.4, 126.1, 125.7, 124.9, 124.4, 122.7, 122.0, 32.3, 30.1, 29.8, 29.4, 23.1, 14.5. HRMS(APCI): calcd for $C_{90}H_{120}N_2S_5$, m/z 1389.8089; found, m/z 1389.8128.

2,6-bis(4-dodecyl-5-(3-(3-dodecylthiophen-2-yl)azulen-1-yl)thiophen-2-yl)-4,8-bis((2-ethylhexyl)oxy)benzo[1,2-b:4,5-b']dithiophene (**BTAz-4**). 5-bromo-3-dodecyl-2-(3-(3-dodecylthiophen-2-yl)azulen-1-yl)thiophene (**5**, 0.213g, 0.3 mmol) and compound 2,6-Bis(trimethylstannyl)-4,8-bis(2-ethylhexyloxy)benzo[1,2-b:4,5-b']dithiophene (0.1 g, 0. 137 mmol) were dissolved in 6 ml toluene. The solution was purged with N_2 for 1 hour. $Pd_2(dba)_3$ (0.0064 g, 0. 007 mmol) and P(o-tolyl)$_3$ (0.0084 g, 0.028 mmol) were added and then slowly heated to 100 °C for 24 hours. After cooling, the reaction mixture was extracted with ethyl ether and the organic layers were collected, washed with water (three times) and dried over magnesium sulfate. After filtration, the volatile toluene and ethyl ether was removed through rotary evaporator. The crude product was chromatographed on silica gel using hexane/DCM (20/5, v/v) as eluent. This was obtained as yellow oil (65%). ^{1}H-NMR (δ, CDCl3): 8.52 (d, 2 H), 8.41 (d, 2 H), 7.96 (s, 2 H), 7.68 (t, 2 H), 7.51 (s, 2 H), 7.37 (d, 2 H), 7.32 (s, 2 H), 7.23 (m, 4 H), 7.11 (d, 2 H), 4.22 (m, 4H), 2.61 (m, 8 H), 1.25 (m, 90 H), 1.07 (t, 8H), 0.98 (t, 8H), 0.88 (m, 16 H). ^{13}C NMR: δ 144.4, 142.0, 141.1, 140.5, 139.5, 139.2, 137.2, 137.1, 136.5, 133.2, 132.8, 132.2, 129.4, 127.8, 124.9, 124.4, 122.7, 121.7, 115.8, 41.1, 32.3, 31.3, 30.9, 30.1, 29.8, 29.6, 29.4, 24.3, 23.6, 23.1, 14.6, 14.5, 11.8. HRMS(APCI): calcd for $C_{110}H_{154}O_2S_6$, m/z 1700.0307; found, m/z 1700.0346.

Results and discussion

The general synthetic procedure for our ICT molecules and controlling molecules is shown in Scheme 2. **BTAz-1** was synthesized via Suzuki Coupling between 1,3-dibromoazulene (**1**) and 4-(4,4,5,5-tetramethyl-1,3,2-dioxaboralan-2-yl)-2,1,3-benzothiadiazole (**2**). Bromination of 1,3-alkylthenyl-azulene (**3**) in solution of chloroform and acetic acid (1:1 v/v) gave compounds **4** and **5**, controlled by the ratio of N-bromosuccinimide (NBS) to compound **3**. Because compound **5** is unstable in air, the coupling reactions of **5** with 2,1,3-Benzothiadiazole- 4,7-bis(boronic acid pinacol ester) (**6**) or **7** were carried out immediately after compound **5** was purified through flash column chromatography, giving compound **BTAz-3** and **BTAz-4** in good yield. Similarly, **BTAz-2** was obtained from reacting **4** with **2**. The chemical structures of compounds were identified by ^{1}H NMR, ^{13}C NMR and HRMS (ESI †).

The push-pull configuration containing alternating electron-rich donor (D) and electron-deficient acceptor (A) along the conjugated backbone is an effective way to obtain narrow band gap chromophores. The incorporation of D/A results in the occurrence of dual-band absorption, and the respective long-wavelength band is attributed to the charge redistribution and low-energy charge-transfer transitions from donor to acceptor.[34-36] As shown in Scheme 1, three ICT systems (**BTAz1-3**) containing both **BT**s and azulenes (**BTAz**s)were designed. In these molecules, **BT**s function as electron acceptors while azulene functions as electron donors in neutral state. **BT** is widely used in various light-harvesting materials and optoelectronic devices because of its good electron-accepting capability due to its heterocyclic group and the observed low band gap in oligomers/polymers containing it.[37,38] **BT** could be protonated in acid solution due to its nitrogen atom. Normally, the protonation ability of molecules can be determined by the computed pKa value.[39] Here, the protonation ability of **BT** in different acid condition was studied by UV-vis spectrum (ESI †). The spectrum indicates **BT** is protonated in concentrated sulfuric acid rather than that in TFA.[40] Interestingly, upon protonation, azulenes are converted to azulenylium ions, which function as new electron-

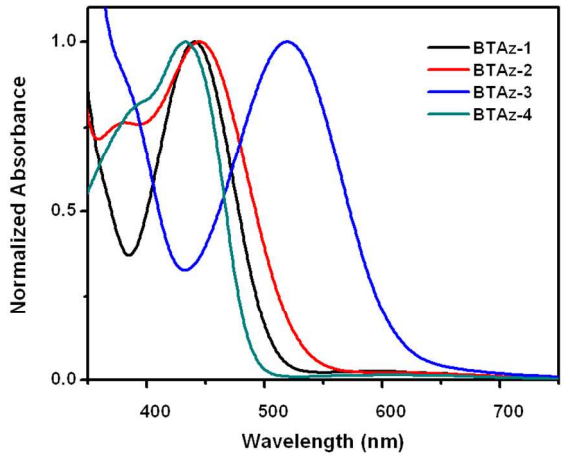

Fig. 1 Normalized optical absorption spectra of **BTAz**s in $CHCl_3$ solution.

accepting center in the ICT system. This effectively shifts the electronic accepting center from **BT**s to azulenes. Azulene is a polar resonance-stabilized non-alternant hydrocarbon with a large dipole moment around 1 D. Electrophilic substitution at C-1 or C-3 in the 5-membered ring of azulene can occur easily to form a very stable aromatic 6π-electron azulenylium ions. Upon protonation, proton is confined in azulene unit, which makes azulene a very strong electron acceptor.[29,41-43] Therefore, the electron accepting center shifts from **BT**s to azulenylium in the ICT molecules upon protonation yield lower energy band gap chromophores with absorption up to middle IR region (2500 nm). To further confirm the ICT effect and verify the shifting of electron accepting center upon protonation, control molecule **BTATB** without obvious electron push-pull characteristic and compound **BTAz-4** containing benzo-dithiophene (**BDT**) were also synthesized as comparison as shown in Scheme 1. The **BDT** unit, which is assumed an entirely planar and symmetrical structure with electron-donating alkoxy group, is more electron rich than donor such as fluorene, thiophene or carbazole, thus promising to be used in D-A system.

As shown in Fig. S2 (ESI †), UV-vis spectrum of compound **BTATB** show a main absorption at 320 nm, which was assigned to π-π* transition of the conjugated oligomer. However, due to the ICT effect in compounds **BTAz**s, **BTAz-1** showed a main absorption at 440 nm (Fig. 1). Compared with **BTATB**, there is about 120 nm red shift, although the conjugated length of **BTAz-1** is obviously shorter than that of **BTATB**. Similar conclusion can be obtained if we compare the UV-vis spectra of **BTAz-1** and **BTAz-4**. Substitution of **BT** with the strong electron donating **BDT** in compound **BTAz-4** leads to no apparent ICT interaction, and thus a blue shift of absorption of **BTAz-4** to 433 nm was observed. Interestingly, we note that **BTAz-3** shows a remarkable red shift than **BTAz-2**. This could be attributed to different D/A arrangement. **BTAz-2** has an A-D-A structure while a D-A-D structure can be found for **BTAz-3**. Therefore, the electron-rich thiophene-azulene moieties in **BTAz-3** facilitate the charge transfer process as electron donors, and thus the D-A-D structure has a stronger charge transfer than A-D-A structure in **BTAz-2** as literature reported previously.[44]

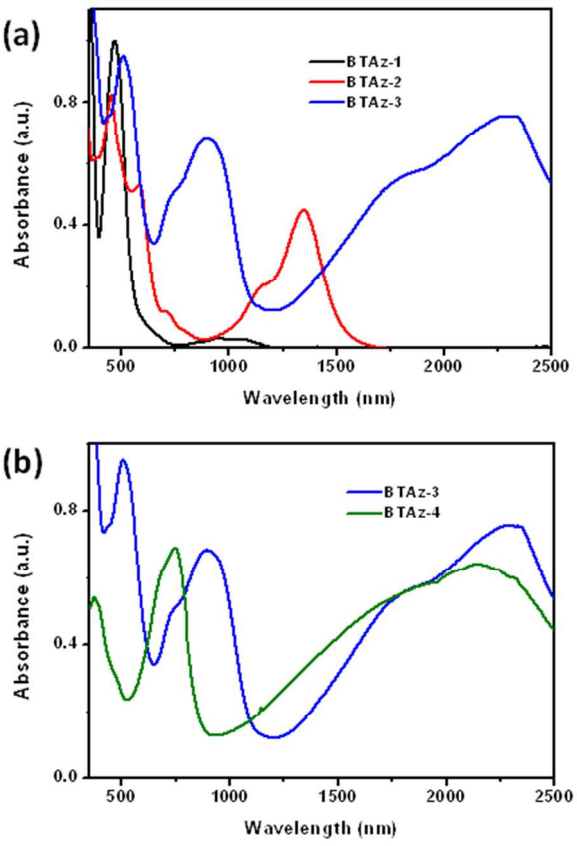

Fig. 2 Optical absorption spectra of **BTAzs** in TFA/$CHCl_3$ (v/v: 3/7) solution.

More significant phenomenon was observed when these monomers were treated with 30% TFA solution. For instance, **BTAz-2** showed two newly formed absorption bands with maxima at 585 and 1344 nm upon protonation (Figure 2a). An additional shoulder at approximately 1150 nm was also observed. The newly formed long wavelength absorption band (~1300 nm) could be attributed to the low-energy transfer occurring from the ground state (S_0) to a charge-separated state (CT). Meanwhile, the absorption in the range of 500 to 1000 nm can be assigned to the electron transfer (ET) in a strong D-A interaction. The excited CT states and ET can both be populated by photo-initiated process.[45]

Compared with **BTAz-2**, **BTAz-1** showed less striking spectra change upon protonation. As shown in Fig. 2a, only a weak transition from S_0 to CT with absorption at around 950 nm can be observed for **BTAz-1** upon protonation. Two main reasons may lead to the weak long wavelength absorption. Firstly, **BT** is intrinsically an electronic acceptor and quite often used as acceptor in ICT molecules. When azulene was protonated to form azulenylium ion which is a strong electronic acceptor, **BT** would be "forced" to become a weak electron donor in protonated **BTAz-1**. Secondly, the weak ICT transition could also be attributed to the structure of **BTAz-1**, in which **BT**s and azulene are connected together directly without spacing. As can be seen from Scheme 1, there is no π-spacer between **BT**s and azulene. Upon protonation, the photoinduced changes in the dipole moment would not be significant, which leads to weak ICT interaction between **BT**s and azulenylium ion. This was

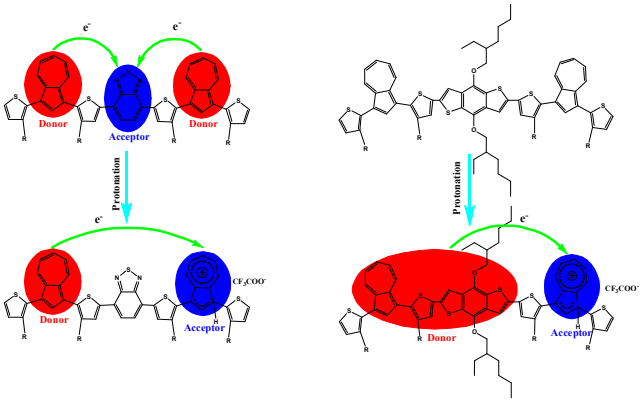

Scheme 3 The donor/acceptor interchange during the protonation of **BTAz-3** (left) and **BTAz-4** (right).

confirmed by our density functional theory (DFT) calculation, which showed that the dipole moment of protonated **BTAz-1** (6.0) is much smaller than that of protonated **BTAz-3** (25.5).

When comparing the UV-vis-NIR spectra of protonated **BTAz-2** and **BTAz-3**, it is shown that **BTAz-3** exhibits a remarkable red shift and enhanced charge transfer, with maximum absorption centers around 2300 nm upon protonation. This could be attributed to the D/A function conversion and the formation of a new ICT transition. For neutral compound **BTAz-3**, obvious ICT transition can be observed with major absorption at 520 nm as shown in Fig. 1, which has been attributed to the D-A-D ICT structure. Upon protonation, one of the azulene was converted into azulenylium ion, forming a stronger electron acceptor. Due to the charge repulsion, it is hard to further protonate the second azulene unit in protonated **BTAz-3**. The un-protonated azulene will remain as electron donor as shown Scheme 3. Compared with the powerful electron-accepting azulenylium ion, previous electron-accepting **BT** unit now mainly functions as π-spacer /linkage in the newly formed ICT system. That is to say, electron drift only occurs from thiophenes and un-protonated azulene to azulenylium ion. Thus, the lengthening of the π-conjugated spacer between donor and acceptor, together with the strong electron donor and acceptor interactions result in a great increase in transition dipole in excited state (25.5 based on DFT simulation), leading to the bathochromic shift of the ICT absorption band of protonated **BTAz-3**.

To further confirm this hypothesis, a control molecule **BTAz-4** as shown in Scheme 1 was designed and synthesized. In **BTAz-4**, benzo-dithiophene (**BDT**), a strong electron donor, was coupled between two azulene units by replacing **BT** in compound **BTAz-3**. Since both azulene and **BDT** have electron-donating properties, no obvious ICT effect was found in neutral **BTAz-4** as shown Fig. 1. Upon protonation, one of azulene unit changed to a strong electron acceptor, protonated **BTAz-4** became an apparent ICT system, in which both the remaining un-protonated azulene and **BDT** functioned as electron donors and the newly formed azulenylium ion functioned as electron acceptor. In addition, as **BDT** is more electron rich than azulene, the electron transfer likely occurs mainly from **BDT** to azulenylium ion. Therefore, charge separation in protonated **BTAz-4** would be less effective than that of **BTAz-3**, and thus hypsochromic shift is expected for protonated **BTAz-4** compared to **BTAz-3**. This was confirmed by our experiment as shown in Fig. 2b. A clear hypsochromic shift for protonated **BTAz-4** can be observed.

Further confirmation regarding our hypothesis comes from

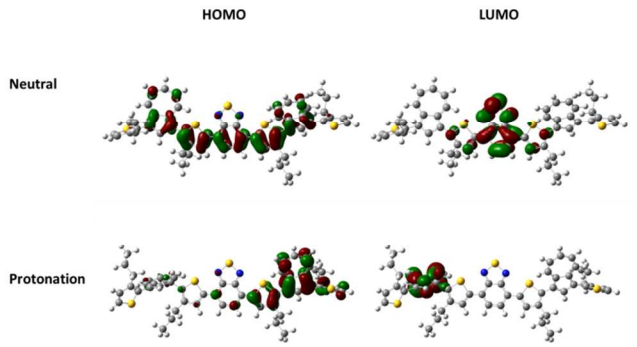

Fig. 3 Spatial distributions of the calculated HOMOs and LUMOs of model compounds **BTAz-3** at different degree of protonation: neutral and protonation.

DFT study of **BTAz**s, in which the spatial distributions of the HOMOs and LUMOs could be obtained (See Fig. 3 and ESI †). DFT calculations agree well with the spectral differences observed experimentally between neutral and protonated states. DFT calculation indicates that protonation process increases the dihedral angle between the thiophene and azulene ring, resulting in a transition from sp^2 carbon to sp^3 carbon. The HOMO in neutral **BTAz-3** is delocalized on the whole conjugated molecule, while LUMO is mainly delocalized on **BT** moiety. Upon protonation, HOMO in protonated **BTAz-3** is mainly delocalized on azulene-thiophene section, and LUMO is delocalized on the azulenylium ion. **BT** in protonated **BTAz-3** acts as a π-conjugated spacer. This explains the large charge separation for protonated **BTAz-3**, and the remarkable spectra change of **BTAz-3** upon protonation. Similar electron density change before and after protonation for **BTAz-2** can also be found from the DFT simulation (See ESI †). For protonated **BTAz-4**, HOMO is mainly delocalized on **BDT** and azulene, while LUMO is mainly localized on the azulenylium ion. Compared with protonated **BTAz-3**, an obvious shorter π-conjugated spacer can be observed in protonated **BTAz-4**.

In order to fully understand the occurrence of two newly appearing peaks in **BTAz-2**, **BTAz-3** and **BTAz-4**, Time dependent (TD)-DFT calculation of excitation energies and oscillation strength was done (ESI †). The first 50 singlet-singlet transition energies were calculated for **BTAz**s under neutral and protonated states and protonated states will be discussed in details. For the excitation energy with oscillator strength (f) less than 0.0001, the possibility of related excited state is quite small and thus would not be considered. The calculated maxima absorption for neutral **BTAz-2**, **BTAz-3** and **BTAz-4** appears at 460 (+16 nm compared to the experimental data of 444 nm), 483 (-37) and 463 (+30) nm, with calculated oscillator strengths of 0.24, 0.08 and 1.60, respectively, which agree well with the experimental data (Fig. 1).

For protonated compounds, the calculation showed two main absorptions that are similar to our experimental results (Fig. 2). For example, only two main absorptions that processing high oscillator strength (f) were found for protonated **BTAz-2** at 980

and 525 nm, similar to the UV-vis-NIR spectra of protonated **BTAz-2** (Fig. 2). Same conclusion can be found in the simulation of protonated **BTAz-3**, in which two wavelengths with high oscillator strength were found at 3242 and 765 nm. For protonated **BTAz-4**, four new peaks with high oscillator strength were found at 4188, 2379, 1665 and 817 nm. Wavelength of 4188 nm is out of our measurement limit, while both wavelength 2379 and 1665 nm are in one experimental observed broad peak for protonated **BTAz-4**. Although the calculated values for protonated compounds are not matched well with experimental data as observed for neutral ones due to the difference between simplified simulation conditions and complicated real protonation process, the simulation results gave a clear conclusion. That is, two new groups of absorption bands were appeared at longer wavelength upon protonation, with the lowest energy transition mainly derived from a combination of the HOMO → LUMO, HOMO-1 → LUMO and HOMO → LUMO+1, and the new absorption in the visible range derived from HOMO-3→LUMO+1 excitation. In addition, according to the calculation, the numbers of accessible excited states for protonated **BTAz-3** and **BTAz-4** are much larger than that of **BTAz-2**. This explains why protonated **BTAz-3** and **BTAz-4** exhibited quite broad peaks that caused by large number of possible energy CT transitions.

Conclusions

In summary, we reported a series of chameleonic conjugated molecules containing azulenes and **BT**s, which showed protonation induced shifting of the electron accepting center and led to remarkable enhancement of the NIR absorption up to 2500 nm. Both the UV-vis-NIR and DFT calculation showed that **BT**s function as electron accepting center in the neutral molecules. However, the electron accepting center shifted to azulenylium ion upon protonation. The ICT transition was influenced by both the arrangement of the donors and acceptors, and the π-conjugated space between the donors and acceptors. This allows a facile way to fine-tune the HOMO-LUMO energy level of the ICT organic chromophores.

Acknowledgements

We acknowledge financial support of this work from the Science and Engineering Research Council (Grant 1123004024) of Agency for Science, Technology and Research of Singapore. T.T. also acknowledges scholarship support from National University of Singapore. DFT calculation was supported by the A*STAR Computational Resource Centre through the use of its high performance computing facilities.

Notes and references

[a] *Department of Materials Science and Engineering, National University of Singapore, 9 Engineering Drive 1, Singapore 117576. E-mail: msehc@nus.edu.sg*

[b] *Institute of Materials Research and Engineering, A*STAR (Agency for Science, Technology and Research), 3 Research Link, Singapore, 117602. Tel: 65 6874 8111; E-mail: wangf@imre.a-star.edu.sg; cb-he@imre.a-star.edu.sg*

[c] *Department of Chemistry, National University of Singapore, 3 Science Drive 3, Singapore 117543.*

† Electronic Supplementary Information (ESI) available: [details of any supplementary information available should be included here]. See DOI: 10.1039/b000000x/

‡ Footnotes should appear here. These might include comments relevant to but not central to the matter under discussion, limited experimental and spectral data, and crystallographic data.

1. M. Luo, H. Shadnia, G. Qian, X. Du, D. Yu, D. Ma, J. S. Wright and Z. Y. Wang, *Chem. Eur. J.,* 2009, **15,** 8902.
2. G. Qian, Z. Zhong, M. Luo, D. Yu, Z. Zhang, Z. Y. Wang and D. Ma, *Adv. Mater.* 2009, **21,** 111.
3. S. T. Meek, E. E. Nesterov and T. M. Swager, *Org. Lett*. 2008, **10,** 2991.
4. E. Bundgaard and F. C. Krebs, *Sol. Energy Mater. Sol. Cell.,* 2007, **91**, 954.
5. A. Yella, H.-W. Lee, H. N. Tsao, C. Yi, A. K. Chandiran, M. K. Nazeeruddin, E. W.-G. Diau, C.-Y. Yeh, S. M. Zakeeruddin and M. Grätzel, *Science,* 2011, **334,** 629.
6. Y. Yao, Y. Liang, V. Shrotriya, S. Xiao, L. Yu and Y. Yang, *Adv. Mater*. 2007, **19,** 3979.
7. S. R. Forrest and M. E. Thompson, Chem. Rev., 2007, **107,** 923.
8. X. Gong, M. Tong, Y. Xia, W. Cai, J. S. Moon, Y. Cao, G. Yu, C.-L. Shieh, B. Nilsson and A. J. Heeger, *Science,* 2009, **325,** 1665.
9. G. Qian and Z. Y. Wang, *Chem. Asian J.,* 2010, **5,** 1006.
10. P.-A. Bouit, G. Wetzel, G. Berginc, B. Loiseaux, L. Toupet, P. Feneyrou, Y. Bretonnière, K. Kamada, O. Maury and C. Andraud, *Chem. Mater.,* 2007, **19,** 5325.
11. J. Roncali, *Chem. Rev.,* 1997, **97,** 173.
12. C. Kitamura, S. Tanaka and Y. Yamashita, *Chem. Mater.,* 1996, **8,** 570.
13. T. Yamamoto, Z.-h. Zhou, T. Kanbara, M. Shimura, K. Kizu, T. Maruyama, Y. Nakamura, T. Fukuda, B.-L. Lee, N. Ooba, S. Tomaru, T. Kurihara, T. Kaino, K. Kubota and S. Sasaki, *J. Am. Chem. Soc.,* 1996, **118,** 10389.
14. S. A. Jenekhe, L. Lu and M. M. Alam, *Macromolecules,* 2001, **34,** 7315.
15. M. Karikomi, C. Kitamura, S. Tanaka and Y. Yamashita, *J. Am. Chem. Soc.* 1995, **117,** 6791.
16. I. Ciofini, T. Le Bahers, C. Adamo, F. Odobel and D. Jacquemin, *J. Phys. Chem. C*, 2012, **116**, 11946.
17. T. L. Tam, H. Li, F. Wei, K. J. Tan, C. Kloc, Y. M. Lam, S. G. Mhaisalkar and A. C. Grimsdale, *Org. Lett.,* 2010, **12,** 3340.
18. S. Ellinger, K. R. Graham, P. Shi, R. T. Farley, T. T. Steckler, R. N. Brookins, P. Taranekar, J. Mei, L. A. Padilha, T. R. Ensley, H. Hu, S. Webster, D. J. Hagan, E. W. Van Stryland, K. S. Schanze and J. R. Reynolds, *Chem. Mater.,* 2011, **23,** 3805.
19. G. L. Gibson, T. M. McCormick and D. S. Seferos, *J. Am. Chem. Soc.,* 2011, **134,** 539.
20. Z. Ning and H. Tian, *Chem. Commun.,* 2009, **37,** 5483.
21. B. Zietz, E. Gabrielsson, V. Johansson, A. M. El-Zohry, L. Sun and L. Kloo, *Phys. Chem. Chem. Phys.*, 2014, **16,** 2251.
22. T. Horiuchi, H. Miura and S. Uchida, *Chem. Commun.,* 2003, **24,** 3036.
23. J. Wiberg, T. Marinado, D. P. Hagberg, L. Sun, A. Hagfeldt and B. Albinsson, *J. Phys. Chem. C,* 2009, **113,** 3881.
24. G. Vellaichamy, V. R. Sergiy and K. K. Jay, *J. Am. Chem. Soc*., 2003**, 125,** 2559.
25. H. A. Staab, J. Weikard, A. Rückemann and A. Schwögler, *Eur. J. Org. Chem.,* 1998, **1998,** 2703.
26. J. Pina, J. S. de Melo, D. Breusov and U. Scherf, *PCCP*, 2013, **15,** 15204.
27. L. Wen, C. L. Heth and S. C. Rasmussen, *PCCP*, 2014, **16**, 7231.
28. T. Tang, T. Lin, F. Wang and C. He, *Polym Chem*, 2014, **5**, 2980.
29. T. Tang, G. Ding, T. Lin, H. Chi, C. Liu, X. Lu, F. Wang and C. He, *Macromol. Rapid Commun.,* 2013, **34,** 431.
30. F. Wang, Y.-H. Lai, N. M. Kocherginsky and Y. Y. Kosteski, *Org. Lett.,* 2003**, 5,** 995.
31. P. Anant, N. T. Lucas and J. Jacob, *Org. Lett.,* **2008,** 10, 5533.
32. M. J. Frisch, G. W. T., H. B. Schlegel, G. E. Scuseria, M. A. Robb, J. R. Cheeseman, G. Scalmani, V. Barone, B. Mennucci, G. A.

Petersson, H. Nakatsuji, M. Caricato, X. Li, H. P. Hratchian, A. F. Izmaylov, J. Bloino, G. Zheng, J. L. Sonnenberg, M. Hada, M. Ehara, K. Toyota, R. Fukuda, J. Hasegawa, M. Ishida, T. Nakajima, Y. Honda, O. Kitao, H. Nakai, T. Vreven, J. A. Montgomery, Jr., J. E. Peralta, F. Ogliaro, M. Bearpark, J. J. Heyd, E. Brothers, K. N. Kudin, V. N. Staroverov, R. Kobayashi, J. Normand, K. Raghavachari, A. Rendell, J. C. Burant, S. S. Iyengar, J. Tomasi, M. Cossi, N. Rega, J. M. Millam, M. Klene, J. E. Knox, J. B. Cross, V. Bakken, C. Adamo, J. Jaramillo, R. Gomperts, R. E. Stratmann, O. Yazyev, A. J. Austin, R. Cammi, C. Pomelli, J. W. Ochterski, R. L. Martin, K. Morokuma, V. G. Zakrzewski, G. A. Voth, P. Salvador, J. J. Dannenberg, S. Dapprich, A. D. Daniels, Ö. Farkas, J. B. Foresman, J. V. Ortiz, J. Cioslowski, and D. J. Fox Gaussian, Inc.; Wallingford CT, 2009.

33. R. E. Stratmann, G. E. Scuseria and M. J. Frisch, *J. Chem. Phys*., 1998, **109**, 8218.
34. Y. Li, *Acc. Chem. Res.,* 2012, **45,** 723.
35. M. Albota, D. Beljonne, J.-L. Brédas, J. E. Ehrlich, J.-Y. Fu, A. A. Heikal, S. E. Hess, T. Kogej, M. D. Levin, S. R. Marder, D. McCord-Maughon, J. W. Perry, H. Röckel, M. Rumi, G. Subramaniam, W. W. Webb, X.-L. Wu and C. Xu, *Science,* 1998, **281,** 1653.
36. J. C. Bijleveld, M. Shahid, J. Gilot, M. M. Wienk and R. A. J. Janssen, *Adv. Funct. Mater.,* 2009, **19,** 3262.
37. G. C. Welch, R. Coffin, J. Peet and G. C. Bazan, *J. Am. Chem. Soc.,* 2009, **131,** 10802.
38. C. R. Belton, A. L. Kanibolotsky, J. Kirkpatrick, C. Orofino, S. E. T. Elmasly, P. N. Stavrinou, P. J. Skabara and D. D. C. Bradley, *Adv. Funct. Mater.,* 2013, **23,** 2792.
39. T. Le Bahers, C. Adamo and I. Ciofini, *Chem. Phys. Lett*., 2009, **472**, 30.
40. H. Kunkely and A. Vogler, *Inorg. Chem. Commun*., 2007, **10**, 1236.
41. J. L. Longridge and F. A. Long, *J. Am. Chem. Soc.,* 1968, **90,** 3088.
42. F. Wang, Y.-H. Lai and M.-Y. Han, *Macromolecules,* 2004, **37**, 3222.
43. F. K. Wang, T. T. Lin, C. B. He, H. Chi, T. Tang and Y. H. Lai, *J. Mater. Chem.,* 2012, **22,** 10448.
44. M. T. Sharbati and F. Emami, *Opt. Express,* 2011, **19,** 3619.
45. Z. R. Grabowski, K. Rotkiewicz and W. Rettig, *Chem. Rev.,* 2003, **103,** 3899.